the plant journal

SEB SOCIETY FOR EXPERIMENTAL BIOLOGY

The Plant Journal (2008) **55**, 1010–1024 doi: 10.1111/j.1365-313X.2008.03570.x

Autophagy regulated by day length determines the number of fertile florets in wheat

Hernán O. Ghiglione[1], Fernanda G. Gonzalez[2,†], Román Serrago[2,3], Sara B. Maldonado[4], Charles Chilcott[5], José A. Curá[1], Daniel J. Miralles[2,3], Tong Zhu[5] and Jorge J. Casal[3,*]

[1]*Bioquímica, Facultad de Agronomía, Universidad de Buenos Aires, Av. San Martín 4453, 1417 Buenos Aires, Argentina,*

[2]*Cátedra de Cerealicultura, Facultad de Agronomía, Universidad de Buenos Aires, Av. San Martín 4453, 1417 Buenos Aires, Argentina,*

[3]*IFEVA, Facultad de Agronomía, Universidad de Buenos Aires and CONICET, Av. San Martín 4453, 1417 Buenos Aires, Argentina ,*

[4]*Departamento de Biodiversidad y Biología Experimental, Facultad de Ciencias Exactas y Naturales, Universidad de Buenos Aires, Av. Intendente Guiraldes s/n, C1428EHA-Buenos Aires, Argentina, and*

[5]*Syngenta Biotechnology Inc., 3054 Cornwallis Road, Research Triangle Park, NC 27709, USA*

Received 11 March 2008; revised 2 May 2008; accepted 15 May 2008; published online 14 July 2008.

[*]For correspondence (fax 5411 4514-8730; e-mail casal@ifeva.edu.ar).

[†]Present address: CONICET, EEA INTA Pergamino, Ruta 32 km 4.5 (B2700WAA), Pergamino, Buenos Aires, Argentina.

Summary

The wheat spikelet meristem differentiates into up to 12 floret primordia, but many of them fail to reach the fertile floret stage at anthesis. We combined microarray, biochemical and anatomical studies to investigate floret development in wheat plants grown in the field under short or long days (short days extended with low-fluence light) after all the spikelets had already differentiated. Long days accelerated spike and floret development and greening, and the expression of genes involved in photosynthesis, photoprotection and carbohydrate metabolism. These changes started while the spike was in the light-depleted environment created by the surrounding leaf sheaths. Cell division ceased in the tissues of distal florets, which interrupted their normal developmental progression and initiated autophagy, thus decreasing the number of fertile florets at anthesis. A massive decrease in the expression of genes involved in cell proliferation, a decrease in soluble carbohydrate levels, and an increase in the expression of genes involved in programmed cell death accompanied anatomical signs of cell death, and these effects were stronger under long days. We propose a model in which developmentally generated sugar starvation triggers floret autophagy, and long days intensify these processes due to the increased carbohydrate consumption caused by the accelerated plant development.

Keywords: wheat, floret development, autophagy, transcriptome.

Introduction

Cereals constitute the most important source of food for humankind. Compared with the model eudicot species *Arabidopsis thaliana* and *Antirrhinum majus*, the inflorescences of grass plants have two distinctive features. First, the flowers are arranged in spikelets, which in turn form composite inflorescences, i.e. a spike (e.g. wheat and maize) or a panicle (e.g. rice, terminal tassel in maize). Second, from outside to inside, the floret contains two leaf-like structures, the lemma and the palea, two lodicules, which occupy the position of the petals, the androecium with three stamens, and the gynoecium with two stigmas. In wheat, spikelet differentiation begins at the transition between vegetative and reproductive development, and ends with formation of the spikelet in the terminal position (terminal spikelet stage). Floret primordia differentiation begins in the central spikelets immediately prior to the terminal spikelet stage, and proceeds downwards and upwards along the spike during all the phases to anthesis (Kirby, 1974). Floret primordia development initiates with differentiation of the anther primordia, and ends when the floret reaches the fertile stage at anthesis, i.e. when the style is curved outwards and the stigmatic branches are spread wide and receive pollen grains (Waddington *et al.*, 1983). While the rice spikelet meristem gives rise to a single floret, the wheat spikelet

meristem has indeterminate development and differentiates up to 12 floret primordia, but at most four or five of these primordia reach the fertile floret stage at anthesis (Kirby, 1974; Langer and Hanif, 1973). The number of fertile florets becomes defined between terminal spikelet stage and anthesis (Figure 1a). The extraordinary diversity of floral structures in angiosperms is only beginning to be explored by a combination of genetic, molecular and morphological tools to gain new insight into gene function. As a result of developing genetics and genomic tools, rice and maize are emerging as models for grasses and monocots in general (Bommert *et al.*, 2005). Wheat is less suitable for genetic studies, and understanding of its development is therefore lagging behind despite its usefulness for investigating the conservation or divergence of mechanisms controlling development, given its closer evolutionary position to rice than to maize (Kellogg, 2001) and the different inflorescence morphology (Bommert *et al.*, 2005). Recent studies describe the changes in the transcriptome of the caryopses after anthesis (Drea *et al.*, 2005; Wilson *et al.*, 2004), but comparable information is lacking for floret development before anthesis, when the number of grains is determined.

In wheat, the transition between vegetative and reproductive development is accelerated by long days (LD) compared to short days (SD; Sawers *et al.*, 2005). Even if applied between terminal spikelet stage and anthesis, LD conditions accelerate the rate of floret development, advance the time when the spike achieves its maximum growth rate, and reduce the number of fertile florets per spikelet at the time of anthesis (Gonzalez *et al.*, 2003, 2005; Miralles *et al.*, 2000). This phenomenon is observed when LD conditions result from extension of SD using low-fluence white light to minimize the impact on photosynthetic input, as well as when SD and LD conditions result from different sowing dates. The number of fertile florets is a key component of grain yield in wheat because it defines the number of grains (Fischer, 1984). To gain insight into the mechanisms that determine the number of fertile florets in wheat, we investigated the transcriptome patterns and the associated physiological processes and developmental anatomy between terminal spikelet stage and anthesis.

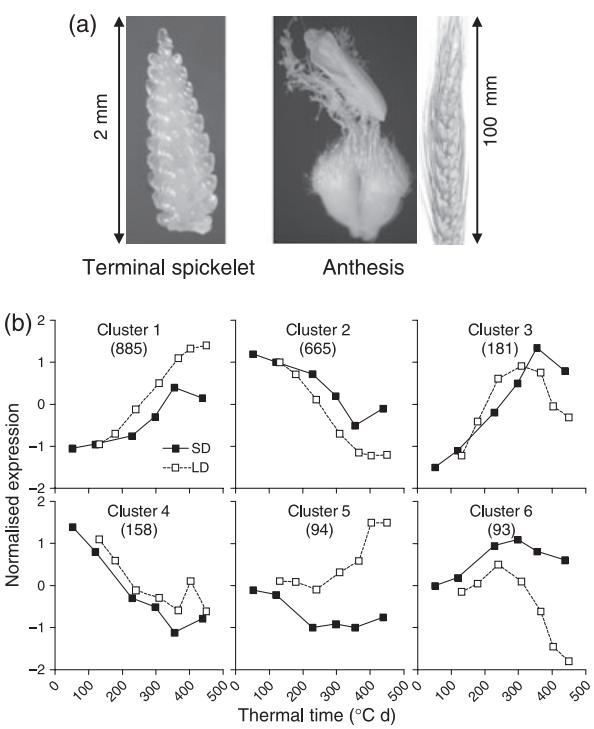

Figure 1. Transcriptome patterns during floret development in wheat.
(a) Photographs of the apex at the terminal spikelet stage, of a fertile floret at anthesis, and of the spike at anthesis. Plants were grown in the field under SD conditions (natural photoperiods). When reproductive development of the main shoot reached the terminal spikelet stage, half of the plants were subjected to LD conditions by 6 h extensions of the natural photoperiod. Samples were collected between the terminal spikelet stage and anthesis.
(b) Mean normalized gene expression of the six most important clusters plotted against thermal time (which measures time as the sum of the daily difference between average temperatures and the base temperature). The number of genes in each cluster is indicated in brackets.

Results

Transcriptome patterns between terminal spikelet and anthesis

Plants of wheat (*Triticum aestivum* L.) were sown in the field under natural SD conditions. When the plants had reached the terminal spikelet stage (Figure 1a), half of the plots were switched to LD conditions, which consisted of a natural photoperiod extended with 6 h of low-fluence white light with a red to far-red ratio similar to that of sunlight. Plant samples were periodically harvested between the terminal spikelet stage and anthesis, i.e. the developmental window during which floral development takes place inside the spikelets. Time course data were plotted against thermal time (which measures time as the sum of the daily difference between average temperatures and a base temperature) rather than chronological time, because thermal time attenuates the impact of temperature fluctuations and makes data more comparable for different years or locations (Trudgill *et al.*, 2005).

RNA samples (which showed no obvious differences with respect to total RNA levels) were used for cRNA synthesis and hybridization to custom-designed Affymetrix GeneChip microarrays containing 38 577 probe sets, including control and experimental probe sets from *Triticum* EST clusters. Images were acquired using an Affymetrix GeneChip scanner and digitized using microarray analysis software. The probe level measurements were summarized using an algorithm. Normalized data (Table S1) were log-transformed and fitted to linear regression models including log harvest time and either light treatment (SD or LD) or log harvest time × light

treatment (interaction) as independent variables. Only the 2127 genes showing significant regression ($q < 0.05$) in each of two independent experiments were used for subsequent analysis. We obtained six clusters containing at least 93 genes (Figure 1b), which account for 2076 of the 2127 significantly affected genes, and three additional clusters (7–9) that include a smaller number of genes (Table S2). All the clusters showed some effect of day length. Genes involved in cellular metabolism dominate clusters 1, 3 and 5; these are mainly carbohydrate metabolism genes (all three clusters) and either photosynthesis-related genes (cluster 1) or lipid metabolism genes (clusters 3 and 5; Table S2). Ribosomal protein genes (cellular metabolism) and genes involved in transcription and RNA processing dominate cluster 2. Clusters 4 and 6, respectively, include relatively large proportions of transcription factors and genes involved in signal transduction, particularly protein kinases. The robust nature of the transcriptome data presented here rests on (i) the smooth temporal patterns, whereby each sample supports the overall trend, (ii) the temporal shift caused by LD conditions compared to SD conditions, which largely parallels the developmental shift described below, (iii) the consistency across 2 years (Figure S1), and (iv) the multiplicity of genes with similar or related function showing the same pattern of response. Below we describe representative genes of each cluster and the related changes in physiology and developmental anatomy.

LD conditions accelerate spike and floret development

After a short lag phase following terminal spikelet development, the spike grows at a constant rate to reach its anthesis size. The linear phase of spike growth occurred earlier under LD versus SD conditions (Figure 2a; Gonzalez *et al.*, 2003, 2005). Under LD conditions, anthesis took place at 450°C days, at which time plants under SD conditions were at the booting stage, at which only the awns are visible 30–50 mm outside the sheath of the uppermost leaf (Figure 2b). Under SD conditions, anthesis occurred at 550°C days (Figure 2a). LD conditions, compared to SD conditions, reduced spike weight at anthesis (Figure 2a). LD conditions also accelerated floret development scored using the developmental scale described by Waddington *et al.* (1983). Figure 2(c,d) shows the evolution of a basal floret of a spikelet located at the central zone of the main shoot spike. LD conditions accelerated the development of both the carpels and the anthers.

Several genes with predicted function in the development of floral organs showed faster increases in expression during floret formation under LD conditions (clusters 1 and 3; Figure 2e and Table S2). The list includes *APETALA2* (*AP2*), a transcription factor involved in the control of flower organ identity and ovule and seed coat development in Arabidopsis (Nilsson *et al.*, 2007; Ohto *et al.*, 2005), *MALE STERILITY 2* (*MS2*), a pollen-specific pectinesterase, which is involved in formation of the pollen wall in Arabidopsis (Aarts *et al.*, 1997), *PLASMA MEMBRANE INTRINSIC PROTEIN 1* (*PIP1*), which is differentially expressed during anther and stigma development in tobacco (Bots *et al.*, 2005), two *ECERIFERUM 1* (*CER1*) genes (Aarts *et al.*, 1995) and *CER6*, which participate in the elimination of very long chain lipids from pollen coats (Fiebig *et al.*, 2000); two *ADHESION OF CALYX EDGES* (*ACE*) genes required for normal floral organ development (Lolle *et al.*, 1998), the family II lipase *EXL3* (Mayfield *et al.*, 2001) that is expressed in the pollen coat of Arabidopsis, two pollen-allergen protein genes (Yennawar *et al.*, 2006), and two *SERINE PROTEASE 1* (*SP1*) genes, which are expressed in the seeds and shoots of rice seedlings and in immature siliques and flowers in Arabidopsis (Yamagata *et al.*, 2000). *OsMADS8* (Lee *et al.*, 2003) and *HvAGAMOUS1* (Kyozuka *et al.*, 2000), which are MADS box genes, two *EF HAND, ABSCISIC ACID*, RESPONSIVE (*EFA27*) genes (Jang *et al.*, 2003) and *LIPOXYGENASE 2* (*LOX2*; van Mechelen *et al.*, 1999) belong to cluster 1, and are expressed in reproductive tissues of rice or barley.

Several genes showed relatively stable expression under SD conditions and increased expression under LD conditions, particularly during the second half of the experimental period (cluster 5, Table S2). These genes include *NO APICAL MERISTEM* (*NAM*), a gene that determines the position of meristems and primordia (Souer *et al.*, 1996), *SERINE CARBOXYPEPTIDASE II-3 PRECURSOR* (*CP-MII.3*), a gibberellic acid-induced gene that is involved in grain development in barley (Dal Degan *et al.*, 1994), and an ascorbate oxidase gene, which is expressed in developing pollen of *Brassica napus* (Albani *et al.*, 1992). *JUBEL2*, a homologue of *BELL1*, which is involved in floral organ development in Arabidopsis (Muller *et al.*, 2001a), showed elevated expression under LD conditions, compared to SD conditions, and a slow reduction with time (cluster 4).

Photosynthesis and carbohydrate metabolism genes

The development of the spike occurs largely inside the tube formed by the sheaths of the leaves, under extremely poor levels of photosynthetic radiation (Figure 3a) and a red to far-red ratio lower than 0.1. Despite these conditions, the chlorophyll content increased during spike development (Figure 3b), and clusters 1 and 5 include a large proportion of genes that encode proteins involved in light-harvesting and photochemical reactions of photosynthesis (Figure 3c and Table S2). The list includes photosystem I antenna proteins, photosystem II core complex proteins, chlorophyll *a*/*b*-binding proteins, various subunits of the photosystem I reaction centre, and thylakoid lumenal 25.6 kDa proteins. Carotenoids are important as accessory antenna pigments and play an important role against oxidative stress. Enzymes involved in carotenoid/xanthophyll

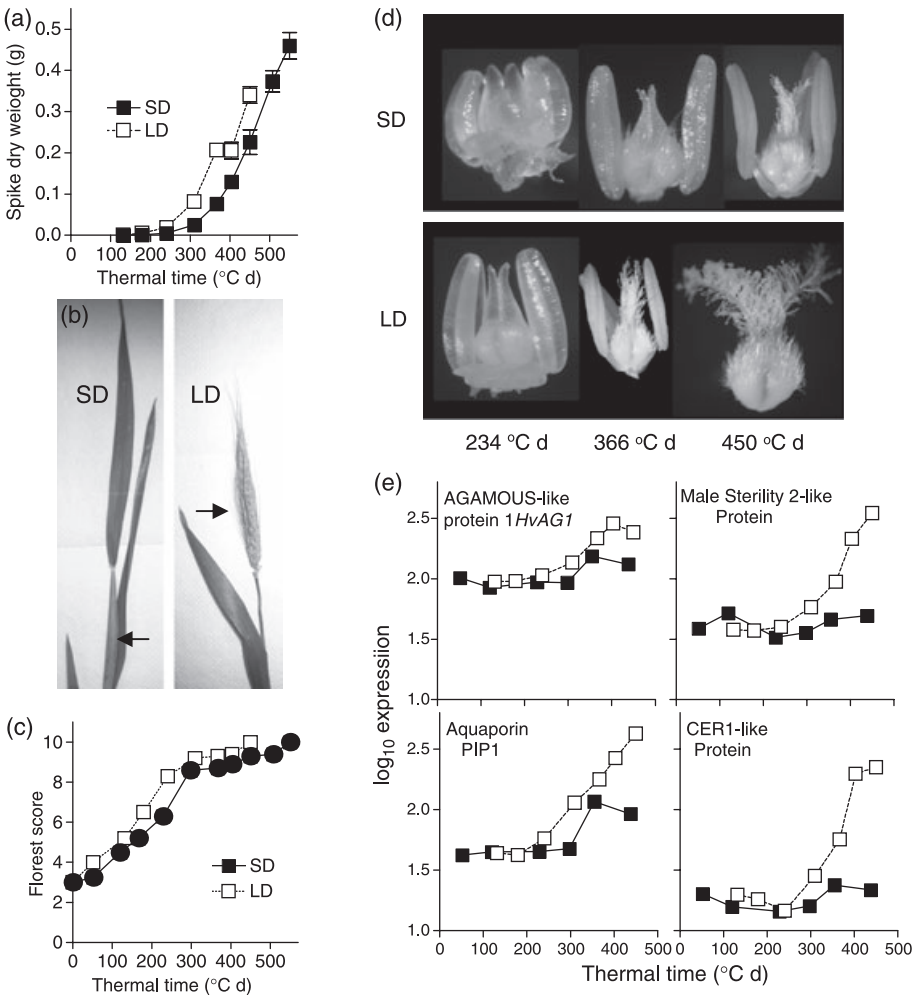

Figure 2. LD conditions, compared to SD conditions, accelerate spike growth and development and expression of genes with a predicted function in floret development.
(a) Dry weight of the spike plotted against thermal time (means ± SE of three replicates).
(b) Detail of the main shoot 450°C days after the beginning of treatment. Note that the spike (indicated by the arrows) has already emerged under LD conditions but not under SD conditions.
(c) LD conditions accelerate floret 1 development compared to SD conditions. Score (Waddington scale) for floret 1 (i.e. the closest to the rachis) of a central spikelet of the main spike, plotted against thermal time (means of three replicates, SE are smaller than the symbols).
(d) Representative florets from central spikelets of the main spike harvested at the indicated thermal times.
(e) Expression patterns of four genes with a predicted function in floral development.

synthesis, such as phytoene synthase, lycopene cyclase, β-carotene hydroxylase and ζ-carotene desaturase are present in cluster 1. Several genes for enzymes involved in the metabolism of flavonoids, which exert a protective function against excess irradiation, are also part of cluster 1. These enzymes include phenylalanine ammonia lyase, cinnamate-4-hydroxylase, chalcone isomerase, 4-coumaroyl: CoA ligase, dihydroflavonol 4-reductase, isoflavone reductase, leucoanthocyanidin dioxygenase and *O*-methyltransferase. A large proportion of the carbon fixation and carbohydrate metabolism genes also showed increased expression. These genes include glyceraldehyde-3-phosphate dehydrogenase, phosphoglycerate kinase and sucrose synthases 1 and 2 (cluster 1; Figure 3d).

Interruption of cell proliferation and floret development

The number of living florets increased gradually during the first half of the period between terminal spikelet stage and anthesis and then declined, determining the number of fertile florets at anthesis. The decline occurred earlier and the final number of fertile florets at anthesis was reduced under LD conditions compared to SD conditions (Figure 4a;.Gonzalez *et al.*, 2003, 2005; Miralles *et al.*, 2000). In Figure 4(b), floret 5 from a central spikelet showed interrupted progression of development before reaching score 6 on the scale of Waddington *et al.* (1983) under either SD or LD conditions. Floret 4, however, reached the fertile stage in SD-treated plants but failed to do so under LD conditions.

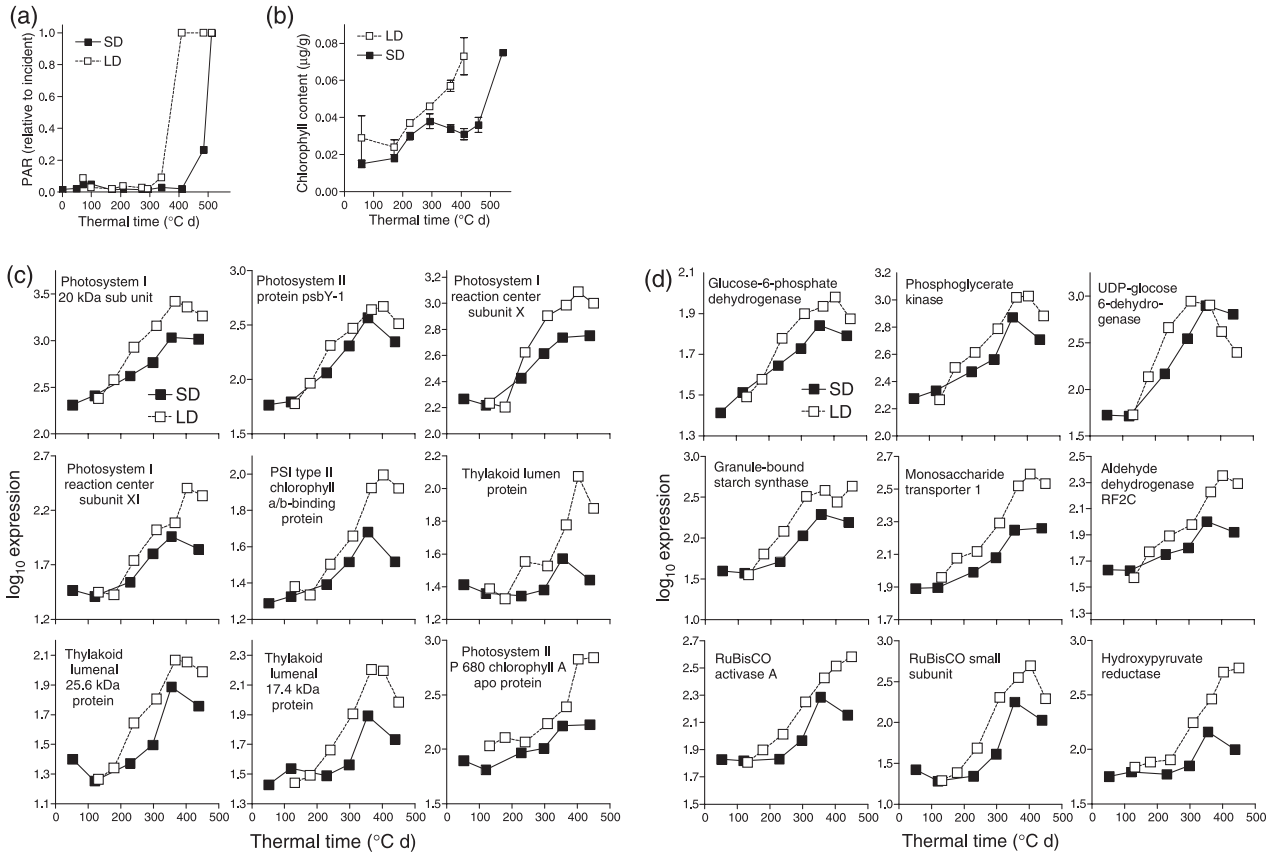

Figure 3. Development of the photosynthetic and carbon metabolism capacity during growth of the spike in a light-depleted environment.
(a) Photosynthetically active radiation (PAR, 400–700 nm) measured with a fibre optic placed at the position of the spike (usually inside the leaf sheath tube) expressed relative to the values for incident radiation.
(b) Chlorophyll levels in the spike (mean ± SE of three replicates).
(c) Expression of representative genes of photosystems I and II in the spike.
(d) Expression of representative genes involved in carbon fixation and metabolism.

This occurred despite the initially faster development under LD conditions (Figure 4b). Progressive degeneration and shrinking of florets may start after reaching a range of developmental stages, including Waddington scores 6 or 7 (Figure 4c) or even lower stages.

Some ovaries aborted at an early stage, with the carpel reaching a thickness of only 8–10 poorly expanded cells (Figure 5a). The ovule showed interruption of normal development at a very early stage: the outer and inner integuments show only incipient development and fail to reach the top of the nucellus. There is no indication of megasporogenesis in the nucellus. Despite the poor development of this ovary, no dividing cells were observed. Some of the cells apparently entered a death program, as evidenced by the lack of a nucleolus, poor staining of chromatin and large vacuoles compared to the relatively small size of the cells (Figure 5a). Some ovaries aborted after further development and megasporogenesis, and showed no dividing cells and the aforementioned signs of a death program in the inner cells of the carpel (not shown). The development of a fertile floret of comparable age is characterized by the presence of more cell layers and more expanded cells (Figure 5b). In the ovule, the nucellus contains the embryo sac and a central vacuole is observed in Figure 5(b). In the carpel, all the tissues are alive, and the cells close to the ovule are densely stained due to the absence of large vacuoles. The latter is also true for integument cells, but other cells are more expanded and vacuolated. The nuclei are very active and cells undergoing mitotic division are frequent (Figure 5c).

Cluster 2, characterized by a gradual decrease in expression levels, included more than 50 histone genes (*H1*, *H2A* and *B*, *H3* and *H4*, Figure 5d and Table S2), and this is consistent with the poor protein staining of chromatin in aborting florets. Histone transcripts are often abundant in tissues undergoing rapid cell division or endo-duplication (Koning *et al.*, 1991), and have been used as markers of cell proliferation in wheat tissues (Drea *et al.*, 2005). Cluster 2 also contains several genes involved in cell proliferation (Figure 5c), such as *REVOLUTA* (Otsuga *et al.*, 2001), *HOMEOBOX GENE 8* (*ATHB-8*; Baima *et al.*, 2001), *PROTEIN KINASE 1* (*APK1*; Ito *et al.*, 1997), *KNOTTED-LIKE*

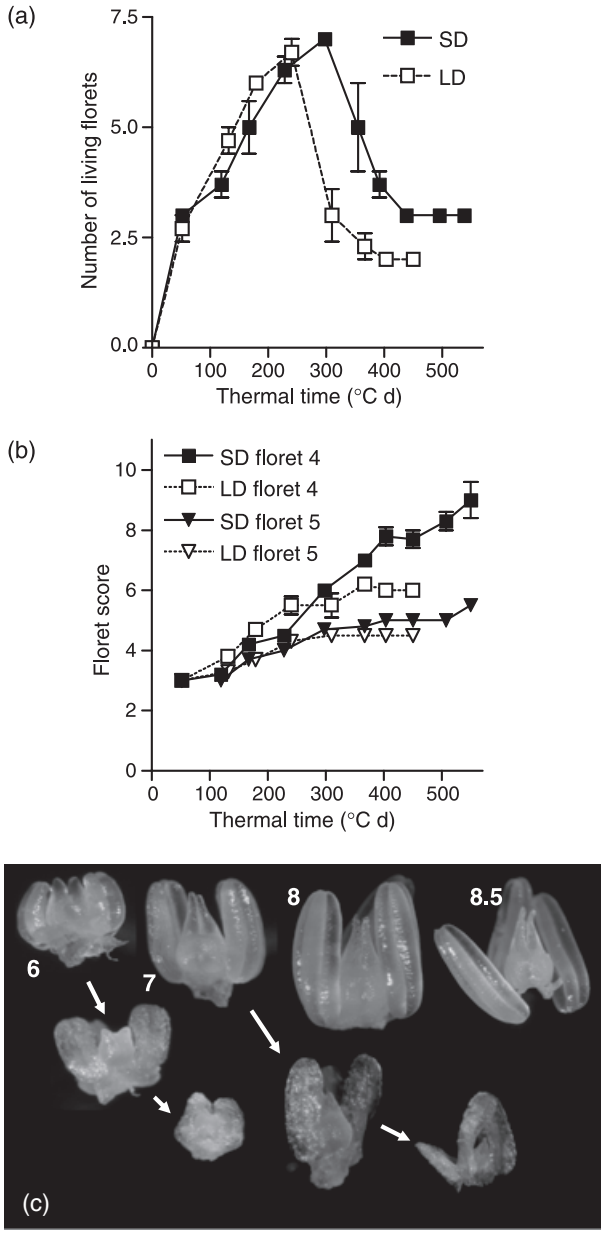

Figure 4. LD conditions increase floret abortion compared to SD conditions.
(a) Number of living florets per spikelet plotted against thermal time. Mean ± SE of three replicates.
(b) Floret score (Waddington scale) plotted against thermal time for florets 4 and 5 of a central spikelet of the main spike. Mean ± SE of three replicates.
(c) Detail of floret development through stages 6, 7, 8 and 8.5 under SD conditions (upper row), indicating the decay of flower organs and flower abortion under LD conditions (arrows).

HOMEOBOX1 (*KNOX1*; Takumi *et al.*, 2000), *HOMEOBOX 1* (*HOX1*; Bellmann and Werr, 1992), *TSO1* (Hauser *et al.*, 2000), *FLAP STRUCTURE-SPECIFIC ENDONUCLEASE 1* (*FEN1*; Kimura *et al.*, 2000), *ARGONAUTE1* (*AGO1*; Kidner and Martienssen, 2005), *PINHEAD* (Lynn *et al.*, 1999), *PESCADILLO*-like (Prisco *et al.*, 2004), *ASY1* (Armstrong *et al.*, 2002; Nonomura *et al.*, 2004), *E2F* and *E2F*-like (*E2L3*; Kosugi and Ohashi, 2002) and *SUPPRESSOR OF FIBRILLARIN 1* (*SOF1*; Jansen *et al.*, 1993). The reduced expression of these genes correlates with the absence of cell division in the increased number of aborting florets. More than 40 ribosomal genes are included in cluster 2 while cluster 1 contained only 11, of which ten are chloroplast ribosomal proteins, and cluster 3 included just one (Table S2). Seven elongation factor genes showed decreased expression (six in cluster 2, one in cluster 4). Finally, genes such as *ERECTA* (Shpak *et al.*, 2004), *ORFX/fw2.2* (Frary *et al.*, 2000) and *SQUAMOSA-LIKE* (Muller *et al.*, 2001b), which are involved in the control of fruit growth and development in other species, showed a relatively stable expression level under SD conditions and decreased expression under LD conditions, particularly during the second half of the experiment (cluster 6, Table S2).

Autophagy in aborting florets

Observation of cells of the ovaries of aborting florets by transmission electron microscopy revealed clear signs of programmed cell death by autophagy rather than passive death or necrosis (Figure 6a–f). The process involves the formation of vacuoles that increase in size, converge and occupy most of the protoplast, except the nucleus. The content of these vacuoles becomes dense because they incorporate autophagic bodies and gradually degrade various organelles. The nucleus shows chromatin condensation and disappearance of the nucleolus. The cell walls suffer modifications resulting in irregular-shaped cells. Finally, the cell, which has been emptied of its protoplast, collapses against the wall of neighbour cells (Figure 5a). Dense globular bodies become evident under electron and light microscopy at early stages of autophagy, and remain throughout the process. These bodies are predicted to be autophagosomes (van Doorn and Woltering, 2005) because a double membrane isolates them from the cytoplasm (Figure 6g, inset). When these vesicles reach maximum density, the membranes are not visible (Figure 6h). At this stage, the bodies move to the surface of the tonoplast (Figure 6d). When the bodies are inside the vacuole, one membrane or no membrane surrounds the dense areas (Figure 6i).

Several genes involved in programmed cell death show increased expression (Figure 6g and Table S2). Cluster 1 includes four genes with similarity to *ACCELERATED CELL DEATH 1* (*LLS1/ACD1*; Yang *et al.*, 2004), which catalyses a key step in chlorophyll degradation (Gray *et al.*, 2004), and two genes with similarity to the *SOLUBLE* N-*ETHYLMALEIMIDE-SENSITIVE FACTOR ATTACHMENT PROTEIN RECEPTOR* (*v-SNARE*; Pal *et al.*, 2006) that is involved in completing fusion between the autophagosome and the vacuole (Ishihara *et al.*, 2001; Sato *et al.*, 1998) and presumably also in maturation of the autophagic vacuole

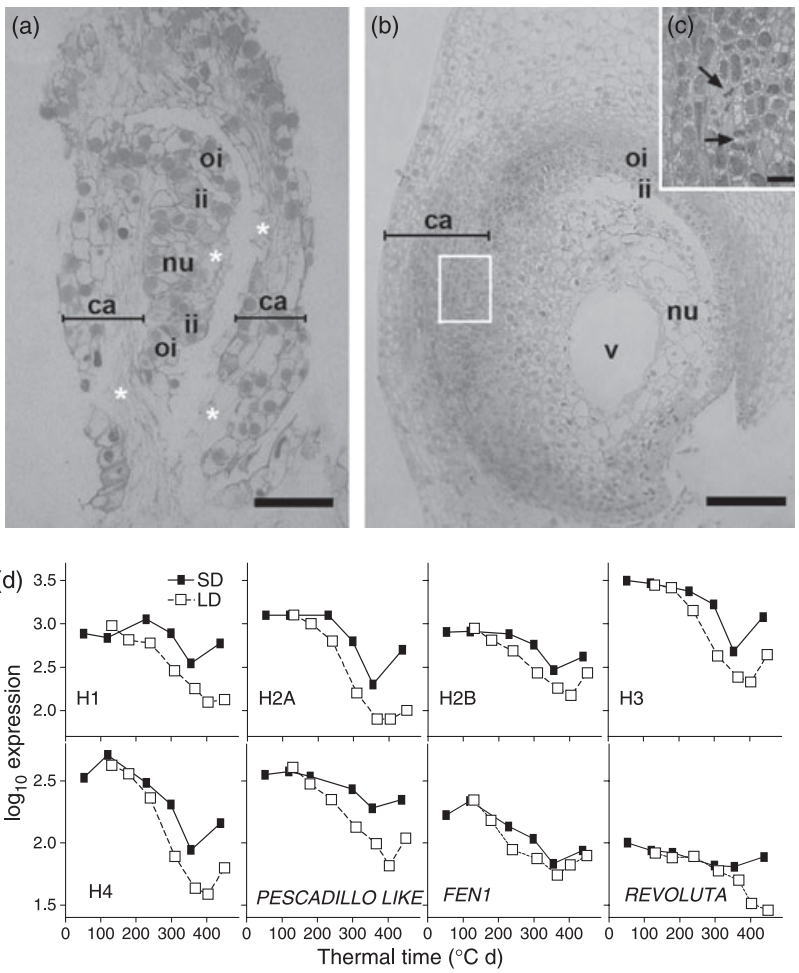

Figure 5. Decreased cell proliferation accompanies floret abortion.
(a) Floret aborted at an early stage of development (note reduced number of cells). ca, carpel; oi, outer integument; ii, inner integument; v, vacuole; nu, nucellus; m, megaspore.
(b) Floret of the same age undergoing normal development.
(c) Detail from (b) showing dividing cells.
(d) Expression of genes involved in cell proliferation.

(Petiot *et al.*, 2002), and *AUTOPHAGY 4* (*APG4*; Tanida *et al.*, 2004) and *APG8*, which are essential for plant autophagy (Yoshimoto *et al.*, 2004) and are involved in several responses to stress and starvation in Arabidopsis (Sláviková *et al.*, 2005). This cluster also includes nine aspartyl proteases, which may be involved in cell death (Syntichaki *et al.*, 2002), and a *PIRIN*-like gene, which is induced in tomato during programmed cell death (Orzaez *et al.*, 2001). *VOLTAGE-DEPENDENT ANION-SELECTIVE CHANNEL PROTEIN* (*VDAC3*; Cesar and Wilson, 2004) and *RAS-RELATED GTP-BINDING PROTEIN 6* (*Rab-6*; Saxena and Kaur, 2006) are included in cluster 3, which shows increased expression levels. Conversely, *APG5* (Matsushita *et al.*, 2006), which plays an essential role in autophagosome formation (Zheng *et al.*, 2004), showed stable expression with slightly higher levels under SD conditions (cluster 9, Table S1). However, an Arabidopsis mutant lacking APG5 showed increased expression of *APG8* (Thompson *et al.*, 2005), suggesting that the expression of these genes might be negatively correlated. *ZINC FINGER PROTEIN RP-8/ PROGRAMMED CELL DEATH PROTEIN 2* (*RP-8*; Owens *et al.*, 1991) showed decreased expression (cluster 2), but its transcriptional upregulation is not universally associated with programmed cell death (Vaux and Hacker, 1995).

In contrast to the increased expression of aspartyl proteases, five genes encoding components of the 20S core particle of the 26S proteasome, the *CONSTITUTIVE PHOTOMORPHOGENESIS 9* (*COP9*) signalosome complex subunit 3 (all in cluster 2) and a 26S proteasome regulatory subunit (cluster 6) showed decreased expression (Figure 7).

Soluble carbohydrate levels

The concentration of soluble carbohydrates decreased markedly between the terminal spikelet stage and anthesis, and this decrease occurred earlier under LD conditions (Figure 8a). In an independent field experiment, we harvested spikes from plants grown under SD conditions approximately 350 and 500°C days after the terminal spikelet stage, and analysed soluble sugars by HPLC. We detected glucose and fructose, but the levels of sucrose were below detection in most samples. The levels of both glucose and fructose decreased between 350 and 500°C days, indicating decay over time (Figure 8b). Samples from plants grown

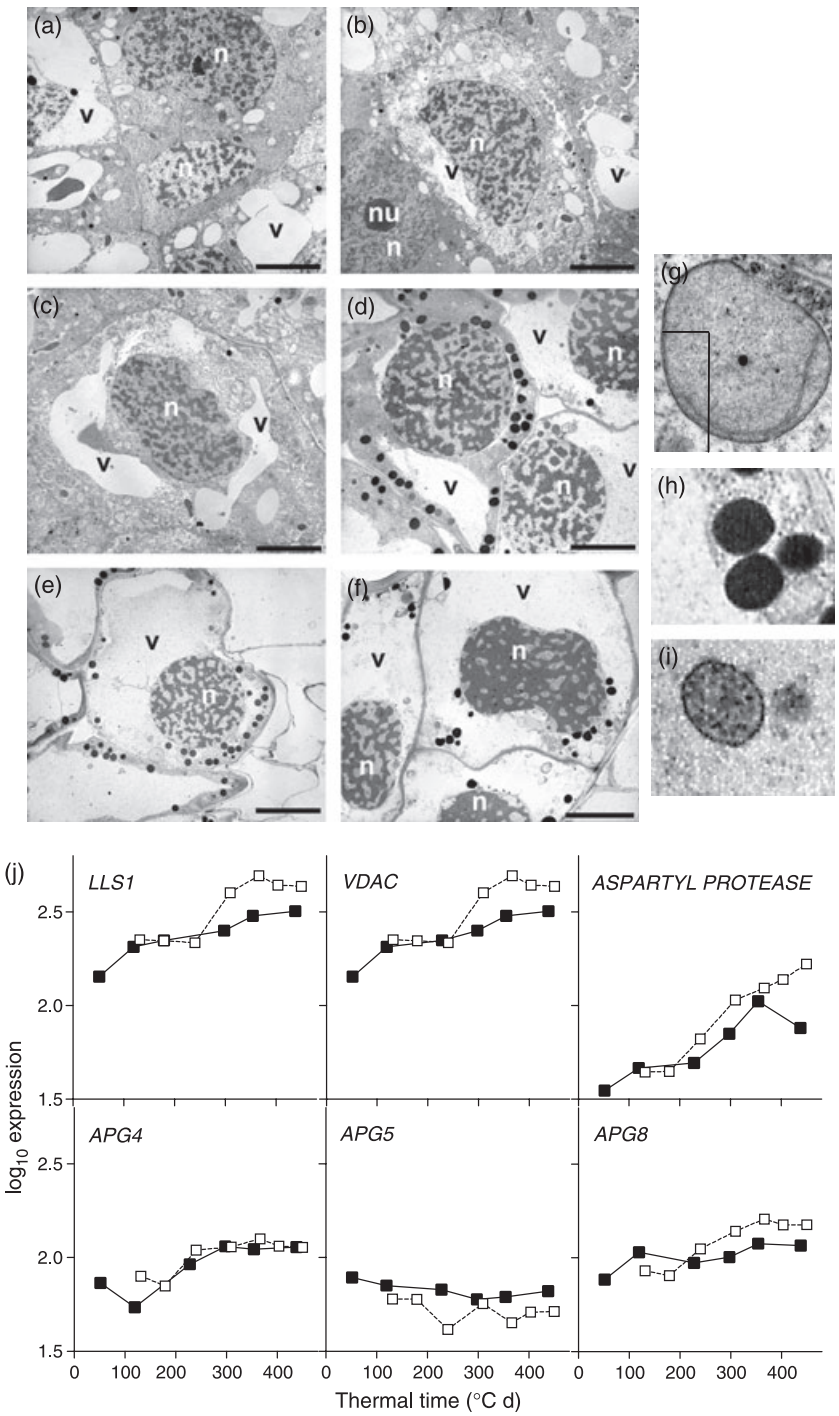

Figure 6. Autophagy is involved in floret abortion.
(a–f) Cells showing different degrees of progression of autophagy.
(g–i) Detail of the autophagosome at various stages in the cytoplasm (g, h) or the vacuole (i).
(j) Expression of genes involved in programmed cell death.

under LD conditions were harvested 350°C days after the terminal spikelet stage, simultaneously with the first set of SD samples. No harvest was performed at 500°C days because LD plants were beyond anthesis at that point. The levels of fructose were reduced in LD plants, confirming the effect of day length (Figure 8b).

Feeding sucrose through the flag leaf during the floret decay period significantly increased the number of fertile florets at anthesis when compared to the polyethylene glycol control at equal water potential (Figure 8c). These manipulative experiments must be interpreted with caution because, as well as acting as a source of carbon, sucrose could also act as a signal. However, at least in principle, the results are consistent with the possibility that the observed decrease in spike sugar levels enhances the decrease in floret number.

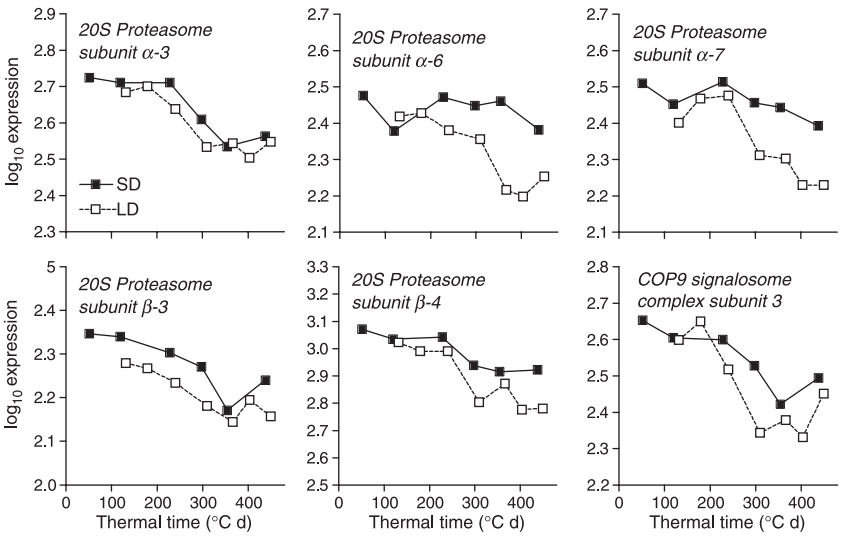

Figure 7. Decreased expression of 26S proteasome-related genes between the terminal spikelet stage and anthesis.

Genes involved in responses to light

Several genes involved in perception and response to light signals showed increased expression during floret development (clusters 1 and 5). They include *HO1*, a haem oxygenase that participates in phytochrome chromophore biosynthesis, *PHOTOTROPIN 1* (Christie *et al.*, 1998), *COP-INTERACTING PROTEIN 7*, which positively regulates light-dependent anthocyanin and chlorophyll accumulation and expression of genes associated with these processes (Yamamoto *et al.*, 1998), and *HEADING DATE 3* (*Hd3a*), which is involved in the photoperiodic control of flowering in rice (Ishikawa *et al.*, 2005).

Hormone-related genes

Three ethylene-forming enzyme (1-aminocyclopropane-1-carboxylate oxidase)-like genes (Yip *et al.*, 1988), *ETHYLENE-INSENSITIVE-3-LIKE* (*OsEIL*; Potuschak *et al.*, 2006), *ETHYLENE RESPONSIVE ELEMENT BINDING PROTEIN* (*EREBP*) and *ETHYLENE RESPONSIVE ELEMENT BINDING FACTOR* (*ERF2*; Fujimoto *et al.*, 2000), are present in cluster 1 (Table S2). The gene corresponding to allene oxide synthase (*AOS*), which is the first enzyme in the lipoxygenase pathway involved in jasmonate biosynthesis (Maucher *et al.*, 2000), and the *LIPOXYGENASE 2* and *3* genes are also included in cluster 1. Auxin flux determines floral organ number and patterning (Nemhauser *et al.*, 2004), and a gene corresponding to the auxin receptor *TRANSPORT INHIBITOR RESPONSE 1* (*TIR1*) gene (Kepinski and Leyser, 2005) showed decreased expression (cluster 2, Table S2).

Discussion

In wheat, many developing florets fail to reach the fertile stage, particularly florets in distal positions within the spikelets but also some florets close to the rachis in basal or apical spikelets within the spike. Floret mortality is more evident in plants grown under LD conditions (SD extended using low-fluence light) than under SD conditions (Figure 4; Gonzalez *et al.*, 2003, 2005; Miralles *et al.*, 2000). Macroautophagy (van Doorn and Woltering, 2005) and not necrosis caused the collapse of the tissues in decaying florets, as indicated by the condensation of chromatin, disappearance of the nucleolus, the formation of numerous vacuoles that converge to form a large vacuole, and the presence of autophagosomes (Figure 6). These cellular patterns correlated with the expression of gene markers of programmed cell death. The cessation of cell division (as evidenced by the reduced number of cell layers and the lack of dividing nuclei) provided an early indication of developmental arrest (Figure 5). This cellular pattern was associated with a massive decrease in the expression of genes involved in cell proliferation. Autophagy is known to be involved in the decay of selected floral tissues (van Doorn and Woltering, 2005). Here we demonstrate that autophagy functions in decay of the entire floret as a mechanism to regulate the number of fertile florets.

Simultaneously with the decay of distal florets, basal florets gradually approach the fertile stage. Increased expression of genes that are known to function in the development of floral structures in Arabidopsis accompanied the developmental progression of basal florets (Figure 2), suggesting that these genes could share functions in both species. Developing florets also showed a gradual increase in chlorophyll content and in the expression of a large number of photosynthetic and photo-protective genes (Figure 3). In etiolated seedlings, the requirement of light to initiate greening and de-etiolation helps to coordinate these events with the unpredictable time at which aerial organs become exposed to photosynthetic light in emerging seedlings. Synthesis of the photosynthetic apparatus in

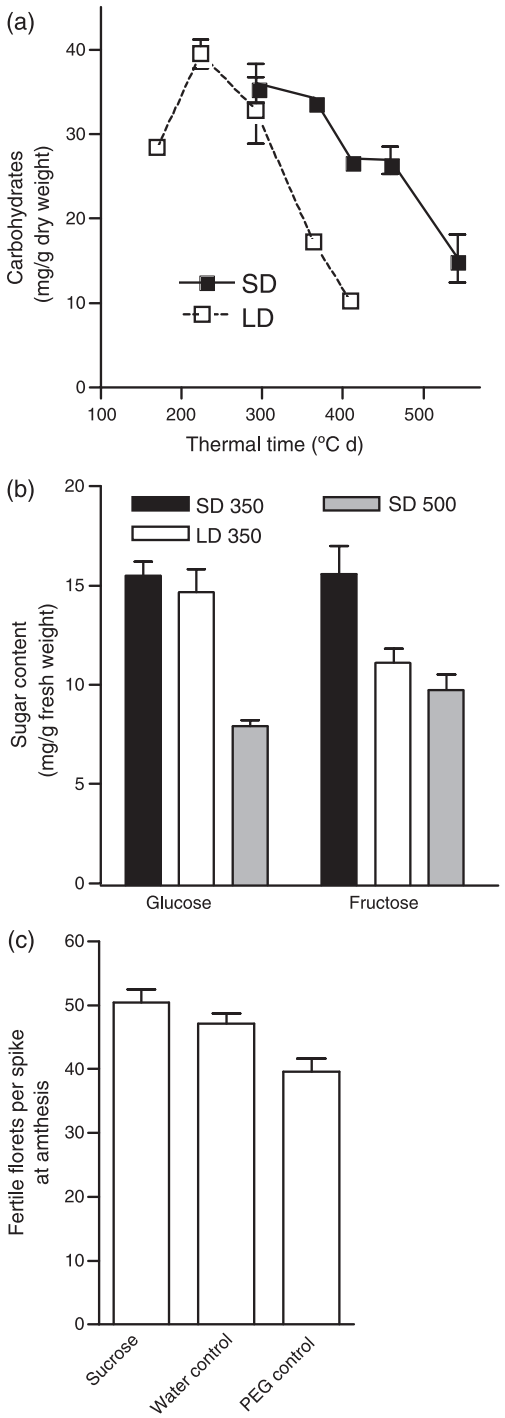

Figure 8. Decreased levels of soluble carbohydrates in the spike and increased number of living florets at anthesis in response to sucrose feeding.
(a) Levels of carbohydrates measured in spike extracts by reaction with anthrone (means ± SE of three replicates).
(b) Levels of sugars detected by HPLC [means ± SE of at least six replicates from an experiment different from that shown in (a)]. Under SD conditions, the spikes were harvested at approximately 350 or 500°C days as indicated, but harvest under LD conditions was at 350°C days only because anthesis occurred before 500°C days.
(c) Effect of sucrose feeding through the flag leaf on the number of living florets at anthesis (means ± SE of at least nine replicates). PEG, polyethylene glycol.

floret tissues appears to follow a developmental program, rather than requiring a light trigger, because it proceeded gradually under the poor light environment created inside the leaf sheath tube and showed no obvious response to the rather abrupt increase in irradiance experienced by the spike close to the occurrence of anthesis (Figure 3). The spike can contribute to the photosynthetic gain and receives a large amount of carbohydrates during grain filling (i.e. after anthesis). Therefore, expression of genes involved in photosynthesis, photo-protection and carbohydrate metabolism pre-anthesis occurs in preparation for the next developmental stage.

LD conditions accelerated the development of basal florets and the rate of floret decay. The expression of marker genes of floral development, photosynthesis, photo-protection, carbohydrate metabolism, cell proliferation and programmed cell death showed a concomitant temporal shift. This scenario is different from the case with *Arabidopsis thaliana*, where photoperiod effects on floral progression are only observed in certain mutant backgrounds (Jeong and Clark, 2005; Okamuro *et al.*, 1996). Several genes corresponding to positive regulators of light signalling showed increased expression between the terminal spikelet stage and anthesis, with a steeper response under LD conditions.

Our data provide insights into the mechanisms that cause autophagy in wheat florets. Stress treatments that cause carbohydrate starvation (darkness, protoplasts with restricted carbon supply) typically induce autophagy (e.g. Xiong *et al.*, 2005). The plants used here were not exposed to stress, but we observed a marked developmentally regulated decrease in soluble carbohydrates, which probably triggered autophagy and floret decay. In accordance with this possibility, feeding sucrose through the flag leaf increased the number of fertile florets at anthesis (Figure 8c). This conclusion is also consistent with the long-standing prediction based on the positive relationship observed between the number of fertile florets and spike dry weight at anthesis, which states that wheat yield is limited by the amount of assimilates allocated to the spike during the last part of the period between the terminal spikelet stage and anthesis (Fischer, 1984). The decrease in soluble carbohydrates could result from the consumption involved in spike growth (Figure 9), as the high rate of spike growth, the decrease in soluble carbohydrates and the decay in living florets all started between 200 and 300°C days. The higher concentration of soluble carbohydrates observed in slow-growing, compared to fast-growing, spikelets (Mishra and Mohapatra, 1987) supports this contention. LD conditions would exacerbate this trend due to the accelerated rate of spike and floret development and hence carbohydrate use. Sugars repress the expression of genes involved in ethylene synthesis and signalling (Price *et al.*, 2004); thus, decreased levels of soluble carbohydrates could trigger the increased expression of ethylene synthesis and signalling genes

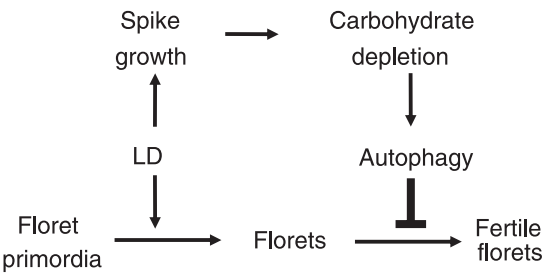

Figure 9. Model of the mechanisms of control of fertile floret number in wheat.

observed in the wheat spike. Male gametophyte survival in rice is inversely related to ethylene levels modulated by inhibitors or ethylene-releasing compounds (Naik and Mohapatra, 1999), and ethylene is able to induce programmed cell death in various tissues in grass plants (Steffens and Sauter, 2005; Young *et al.*, 1997), suggesting that high levels of ethylene may be necessary for the occurrence of autophagy in dying florets. Genes involved in jasmonate synthesis or signaling also showed increased expression between the terminal spikelet stage and anthesis, and could act synergistically with ethylene-related genes (Lorenzo *et al.*, 2003). Based on analysis of co-expressed gene sets, Sreenivasulu *et al.* (2006) proposed that the induction of programmed cell death in the pericarp of barley seeds is mediated by jasmonate and ethylene via EREBP transcription factors. Several genes related to COP9 and the 26S proteasome showed decreased expression, and regulated reduction of the activity of the 26S proteasome might be a developmental trigger involved in the initiation of programmed cell death, via reduced proteolytic degradation of death triggers (Kim *et al.*, 2003). However, COP9 could also participate in the modulation of light effects and in the regulation of floret development (Wang *et al.*, 2003). In the present work, transcriptome data are used mainly as molecular markers, which, in combination with anatomical, physiological and biochemical observations, help to uncover the processes that regulate the number of fertile florets in wheat. However, in addition to this conservative use, the data will be helpful as a resource in the future search for transcription factors that are able to regulate the pace of floret development and hence floret survival under various photoperiods (Sawers *et al.*, 2005).

Experimental procedures

Plant material

Plants of wheat (*Triticum aestivum*) cultivar Buck Manantial were sown on 16 July 2003, 20 July 2004 and 22 July 2005 at a density of 240 plants per m^2 at the experimental field of the Faculty of Agronomy, University of Buenos Aires (37º34′S, 58º20′W), on a silt clay loam classified as Vertic Argiudol (United States Department of Agriculture taxonomy). Urea was added at the start of tillering and at the time of stem elongation at a rate of 60 kg of nitrogen per hectare in each case. Weeds were controlled manually, and fungicides and pesticides were applied to prevent fungal diseases and insect damage. Rainfall was complemented throughout the crop cycle by irrigation. Each replicate plot consisted of nine 1.2 m rows.

Photoperiod treatments

Photoperiod treatments were applied only during the spike growth period, i.e. between the terminal spikelet stage and anthesis. Plants were either exposed to the natural photoperiod of the growing season (approximately 12.5 h) or to natural photoperiods followed by a light extension of 6 h provided by a mixture of incandescent and fluorescent lamps. The photosynthetic photon flux density (400–700 nm) of the supplementary light was 4 μmol m^{-2} sec^{-1} (measured on top of the canopy using a LI-COR Inc. (www.licor.com) quantum sensor) and the red to far-red ratio was 1.17 (measured using a SKR 110 660/730 sensor, Skye Instruments Ltd, www.skyeinstruments.com). Thus, the extension made a negligible contribution to photosynthesis and did not significantly alter the natural red to far-red ratio.

RNA samples

The main shoots of field-grown plants were harvested at midday twice a week. The spike was dissected immediately after harvest using a binocular microscope (Leica MZ6, www.leica.com) in a laboratory located close to the field plots, and samples were stored in liquid nitrogen. RNA was extracted from the main shoot spike using a NucleoSpin® RNA plant kit (Macherey-Nagel, www.macherey-nagel.com). RNA quality was assessed by gel electrophoresis.

Custom-designed wheat GeneChip microarray

The custom-designed wheat GeneChip® (Affymetrix, www.affymetrix.com) has unique probe sets for 38 514 EST clusters of *Triticum* spp. Each probe set has 13 perfect matched probes, each occupying 18×18 μm^2 of space. In addition to the wheat probe sets, various control probe sets are also present in the chip. The hybridization images were obtained and processed by Affymetrix MAS 5.0. hybridization signals of perfect matched probes of a set were condensed into a single index based on 72 percentile using a custom script. The condensed data are globally normalized so that the average probe set signal intensity of all arrays equals to 100. The background signal was determined as 54.70, based on an average hybridization index of 27.90 and a standard deviation of 13.4 determined by measuring 27 negative control probe sets in 19 samples. The technical reproducibility is high, with an average coefficient of correlation of 0.9718 (CV = 0.0298%, $n = 91$). The linear dynamic range is >500-fold between 0.4 and 400 pM. The detection sensitivity for the array was determined as 0.8 pM based on analysis of a dilution series of four bacterial spike control genes.

Transcriptome statistics

Two independent experiments performed in different years were used for transcriptome analysis. In each of the experiments, a single

microarray was used for each harvest time and photoperiod condition in combination with frequent sampling. This design allows detailed description and a robust statistical analysis of the time course of expression of those genes that show gradual changes with time. The trade-off in this choice is that the design has no power to support statistically the temporal pattern of those genes showing peaks of expression restricted to a single harvest time. Preliminary inspection of the data by clustering analysis (De Smet *et al.*, 2002) showed that >14 000 genes grouped in 51 clusters whose expression values changed gradually through the sampling period with apparent differences between SD and LD conditions (data not shown). None of these clusters showed peaks restricted to one harvest time, and therefore no significant loss of information is predicted.

For each experiment, normalized data were log-transformed and fitted to linear regression models including log harvest time and either light treatment (SD conditions = 0, LD conditions = 1) or log harvest time × light treatment as independent variables. The *P* values were transformed into probabilities of false positives among selected genes (*q*; Storey and Tibshirani, 2003). A gene was regarded as significantly affected by time and/or photoperiod when *q* values were lower than 0.05 in each of the two independent experiments. Thus, the probability of false positives among these genes is lower than 0.05. We prioritized conservative selection of genes by introducing this very stringent statistical cut-off, but this means that non-selected genes present in the microarray cannot be regarded as not significantly affected without further inspection.

Clusters (De Smet *et al.*, 2002) include only the genes significant affected in both experiments, but are based on the first of the two field experiments, which included more samples. The probability for a gene to be included in a given cluster was set at 80%, and minimum number of genes required per cluster was five, because more stringent sorting resulted in large number of clusters with relatively small differences in pattern.

Physiological and biochemical measurements

The thermal time since the terminal spikelet stage was calculated as the cumulative sum of the differences between the daily mean air temperature minus the base temperature (0°C). The dry weight of the spike was measured after drying samples collected simultaneously with those used for the analysis of gene expression for at least 3 days at 62°C. The scale described by Waddington *et al.* (1983) was used to assign a floret score. Total chlorophyll content was quantified from fresh samples (1 g) extracted in acetone (2 ml) in darkness at −20°C as described previously (Arnon, 1949). Soluble carbohydrates were measured in extracts from 0.1 g ground dry tissue according to the methodology proposed by Yemm and Willis (1954) using glucose standards. Soluble sugars were determined by HPLC as described previously (Lee *et al.*, 2007), but the spikes were ground in liquid nitrogen before washing with boiling ethanol, and pigments were extracted with chloroform after passing the concentrate through an ultrafilter membrane. HPLC was performed on an Agilent 1100 with an Agilent Zorbax carbohydrate analysis column (www.agilent.com), a refraction index detector, and a flow rate of 1.4 ml min^{-1} of acetonitrile:water (75:25) at 30°C.

For sucrose-feeding experiments, the plants were grown in pots in a glasshouse. The tip of the unfolded flag leaf was trimmed immediately prior to the booting stage (i.e. when the spike has approximately half of its final size and the number of living florets is decreasing) and placed inside 10 ml glass tubes containing either distilled water, sucrose (0.2 M) or polyethylene glycol (to produce the same osmotic potential as the sucrose solution; Figure S2). The solutions were replaced and the distal part of the flag leaf (immersed in the solutions) was removed every other day.

Characterization of the light environment reaching the spike

A fibre optic of 0.5 mm diameter (Poly-Optics Inc., www.fiberopticlight.com) was connected to the tip (after removing the cosine corrector) of the fibre optic probe of an Ocean Optics (www.oceanoptics.com) spectroradiometer. Plants were harvested and taken to the laboratory, where the free end of the fibre optic was transversely introduced into the leaf sheath tube at the position corresponding to the height reached by the spike. The identification of spike height often required destructive observation of shoots from plants grown simultaneously in the field plots. The light source was an incandescent lamp placed perpendicular to the main axes of the shoot, i.e. facing the tip of the fibre optics. The results of repeated scans were averaged and are expressed relative to the light reaching the fibre optic tip when not buried inside the plant tissues.

Microscopy

Flowers were fixed in 0.5% v/v glutaraldehyde and 2.5% v/v paraformaldehyde in 0.1 M phosphate buffer, pH 7.2, at 4°C for 3 h. The tissue was washed three times with phosphate buffer and then dehydrated in an ethanol series with 50, 60, 70 and 90% ethanol (30 min each). The samples were then embedded in LR-White resin (Polyscience, www.polyscience.com) and stained with toluidine blue O (Sigma, http://www.sigmaaldrich.com/). Sections (1 μm thick) were mounted on glass slides using poly-L-lysine (Sigma-Aldrich) and stained with toluidine blue O.

For electron microscopy, ultra-thin sections were prepared using a Reichert-Jung (www.reichertms.com) ultramicrotome, mounted on nickel grids, and subsequently stained with uranyl acetate and lead citrate. Sections were then examined using a Zeiss EM 109 turbo transmission electron microscope (http://www.zeiss.com/).

Acknowledgements

This work was supported by grants from the Consejo Nacional de Investigaciones Científicas y Técnicas (number PIP 5958), the Agencia Nacional de Promoción Científica y Tecnológica (number BID 1728/OC-AR PICT 11631), and the University of Buenos Aires (number G021) to J.J.C., and from Syngenta to T.Z.

Supporting Information

Additional supporting information may be found in the online version of this article.

Figure S1. Gene expression in year 2 plotted against gene expression in year 1 for each date and SD/LD condition.

Figure S2. Experimental set-up for in sucrose feeding experiments.

Table S1. Log expression values during the 2 years of field experimentation.

Table S2. Clusters of genes showing significant changes in expression during the 2 years of field experimentation.

Please note: Blackwell publishing are not responsible for the content or functionality of any supporting materials supplied by the authors. Any queries (other than missing material) should be directed to the corresponding author for the article.

References

Aarts, M.G.M., Keijzer, C.J., Stiekema, W.J. and Pereira, A. (1995) Molecular characterization of the CER1 gene of Arabidopsis involved in epicuticular wax biosynthesis and pollen fertility. *Plant Cell*, **7**, 2115–2127.

Aarts, M.G., Hodge, R., Kalantidis, K., Florack, D., Wilson, Z.A., Mulligan, B.J., Stiekema, W.J., Scott, R. and Pereira, A. (1997) The *Arabidopsis MALE STERILITY 2* protein shares similarity with reductases in elongation/condensation complexes. *Plant J.* **12**, 615–623.

Albani, D., Sardana, R., Robert, L.S., Altosaar, I., Arnison, P.G. and Fabijanski, S.F. (1992) A *Brassica napus* gene family which shows sequence similarity to ascorbate oxidase is expressed in developing pollen. Molecular characterization and analysis of promoter activity in transgenic tobacco plants. *Plant J.* **2**, 331–342.

Armstrong, S.J., Caryl, A.P., Jones, G.H. and Franklin, F.C. (2002) Asy1, a protein required for meiotic chromosome synapsis, localizes to axis-associated chromatin in *Arabidopsis* and *Brassica*. *J. Cell Sci.* **15**, 3645–3655.

Arnon, D.I. (1949) Copper enzymes in isolated chloroplast. Polyphenoloxidase in *Beta vulgaris*. *Plant Physiol.* **24**, 1–15.

Baima, S., Possenti, M., Matteucci, A., Wisman, E., Altamura, M.M., Ruberti, I. and Morelli, G. (2001) The Arabidopsis ATHB-8 HD-zip protein acts as a differentiation-promoting transcription factor of the vascular meristems. *Plant Physiol.* **126**, 643–655.

Bellmann, R. and Werr, W. (1992) Zmhox1a, the product of a novel maize homeobox gene, interacts with the Shrunken 26 bp feedback control element. *EMBO J.* **11**, 3367–3374.

Bommert, P., Satoh-Nagasawa, N., Jacson, D. and Hirano, H.-Y. (2005) Genetics and evolution of inflorescence and flower development in grasses. *Plant Cell Physiol.* **46**, 69–78.

Bots, M., Feron, R., Uehlein, N., Weterings, K., Kaldenhoff, R. and Mariani, T. (2005) PIP1 and PIP2 aquaporins are differentially expressed during tobacco anther and stigma development. *J. Exp. Bot.* **56**, 113–121.

Cesar, M.C. and Wilson, J.E. (2004) All three isoforms of the voltage-dependent anion channel (VDAC1, VDAC2, and VDAC3) are present in mitochondria from bovine, rabbit, and rat brain. *Arch. Biochem. Biophys.* **15**, 191–196.

Christie, J.M., Reymond, P., Powell, G.K., Bernasconi, P., Raibekas, A.A., Liscum, E. and Briggs, W.R. (1998) *Arabidopsis* NPH1: a flavoprotein with the properties of a photoreceptor for phototropism. *Science*, **282**, 1698–1701.

Dal Degan, F., Rocher, A., Cameron-Mills, V. and von Wettstein, D. (1994) The expression of serine carboxypeptidases during maturation and germination of the barley grain. *Proc. Natl Acad. Sci. USA*, **16**, 8209–8213.

De Smet, F., Mathys, J., Marchal, K., Thijs, G., De Moor, B. and Moreau, Y. (2002) Adaptive quality-based clustering of gene expression profiles. *Bioinformatics*, **18**, 735–746.

van Doorn, W.G. and Woltering, E.J. (2005) Many ways to exit? Cell death categories in plants. *Trends Plant Sci.* **10**, 117–122.

Drea, S., Leader, D.J., Arnold, B.C., Shaw, P., Dolan, L. and Doonana, J.H. (2005) Systematic spatial analysis of gene expression during wheat caryopsis development. *Plant Cell*, **17**, 2172–2185.

Fiebig, A., Mayfield, J.A., Miley, N.L., Chau, S., Fischer, R.L. and Preuss, D. (2000) Alterations in *CER6*, a gene identical to *CUT1*, differentially affect long-chain lipid content on the surface of pollen and stems. *Plant Cell*, **12**, 2001–2008.

Fischer, R.A. (1984) Wheat. In *Potential Productivity of Field Crops Under Different Environments* (Smith, W.H. and Banta, J.J., eds). Los Baños: IRRI, pp. 129–154.

Frary, A., Nesbitt, T.C., Grandillo, S., Knaap, E., Cong, B., Liu, J., Meller, J., Elber, R., Alpert, K.B. and Tanksley, S.D. (2000) *fw2.2*: a quantitative trait locus key to the evolution of tomato fruit size. *Science*, **289**, 85–88.

Fujimoto, S.Y., Ohta, M., Usui, A., Shinshi, H. and Ohme-Takagi, M. (2000) Arabidopsis ethylene-responsive element binding factors act as transcriptional activators or repressors of GCC box-mediated gene expression. *Plant Cell*, **12**, 393–404.

Gonzalez, F.G., Slafer, G.A. and Miralles, D.J. (2003) Floret development and spike growth as affected by photoperiod during stem elongation in wheat. *Field Crops Res.* **81**, 29–38.

Gonzalez, F.G., Slafer, G.A. and Miralles, D.J. (2005) Floret development and survival in wheat plants exposed to contrasting photoperiod and radiation environments during stem elongation. *Funct. Plant Biol.* **32**, 189–197.

Gray, J., Wardzala, E., Yang, M., Reinbothe, S., Haller, S. and Pauli, F. (2004) A small family of LLS1-related non-heme oxygenases in plants with an origin amongst oxygenic photosynthesizers. *Plant Mol. Biol.* **54**, 39–54.

Hauser, B.A., He, J.Q., Park, S.O. and Gasser, C.S. (2000) TSO1 is a novel protein that modulates cytokinesis and cell expansion in *Arabidopsis*. *Development*, **127**, 2219–2226.

Ishihara, N., Hamasaki, M., Yokota, S., Suzuki, K., Kamada, Y., Kihara, A., Yoshimori, T., Noda, T. and Ohsumi, Y. (2001) Autophagosome requires specific early Sec proteins for its formation and NSF/SNARE for vacuolar fusion. *Mol. Biol. Cell*, **12**, 3690–3702.

Ishikawa, R., Tamaki, S., Yokoi, S., Inagaki, N., Shinomura, T., Takano, M. and Shimamoto, K. (2005) Suppression of the floral activator *Hd3a* is the principal cause of the night break effect in rice. *Plant Cell*, **17**, 3326–3336.

Ito, T., Takahashi, N., Shimura, Y. and Okada, K. (1997) A serine/threonine protein kinase gene isolated by an in vivo binding procedure using the *Arabidopsis* floral homeotic gene product, AGAMOUS. *Plant Cell Physiol.* **38**, 248–258.

Jang, C.S., Lee, M.S., Kim, J.Y., Kim, D.S. and Seo, Y.W. (2003) Molecular characterization of a cDNA encoding putative calcium binding protein, HvCaBP1, induced during kernel development in barley (*Hordeum vulgare* L.). *Plant Cell Rep.* **22**, 64–70.

Jansen, R., Tollervey, D. and Hurt, E.C. (1993) A U3 snoRNP protein with homology to splicing factor PRP4 and G beta domains is required for ribosomal RNA processing. *EMBO J.* **12**, 2549–2558.

Jeong, S. and Clark, S.E. (2005) Photoperiod regulates flower meristem development in *Arabidopsis thaliana*. *Genetics*, **169**, 907–915.

Kellogg, E.A. (2001) Evolutionary history of the grasses. *Plant Physiol.* **125**, 1198–1205.

Kepinski, S. and Leyser, O. (2005) The Arabidopsis F-box protein TIR1 is an auxin receptor. *Nature*, **435**, 446–451.

Kidner, C.A. and Martienssen, R.A. (2005) The role of ARGONAUTE1 (AGO1) in meristem formation and identity. *Dev. Biol.* **15**, 504–517.

Kim, M., Ahn, J.-W., Jin, U.-H., Choi, D., Paek, K.-H. and Pai, H.-S. (2003) Activation of the programmed cell death pathway by inhibition of proteasome function in plants. *J. Biol. Chem.* **278**, 19406–19415.

Kimura, S., Ueda, T., Hatanaka, M., Takenouchi, M., Hashimoto, J. and Sakaguchi, K. (2000) Plant homologue of flap endonuclease-1: molecular cloning, characterization, and evidence of expression in meristematic tissues. *Plant Mol. Biol.* **42**, 415–427.

Kirby, E.J.M. (1974) Ear development in spring wheat. *J. Agric. Sci.* **82**, 437–447.

Koning, A.J., Tanimoto, E.Y., Kiehne, K., Rost, T. and Comai, L. (1991) Cell-specific expression of plant histone H2A genes. *Plant Cell*, **3**, 657–665.

Kosugi, S. and Ohashi, Y. (2002) E2Ls, E2F-like repressors of Arabidopsis that bind to E2F sites in a monomeric form. *J. Biol. Chem.* **277**, 16553–16558.

Kyozuka, J., Kobayashi, T., Morita, M. and Shimamoto, K. (2000) Spatially and temporally regulated expression of rice MADS box genes with similarity to Arabidopsis class A, B and C genes. *Plant Cell Physiol.* **41**, 710–718.

Langer, R.H.M. and Hanif, M. (1973) A study of floret development in wheat (*Triticum aestivum* L.). *Ann. Bot.* **37**, 743–751.

Lee, S., Jeon, J.S., An, K., Moon, Y.H., Lee, S., Chung, Y.Y. and An, G. (2003) Alteration of floral organ identity in rice through ectopic expression of *OsMADS16*. *Planta*, **217**, 904–911.

Lee, H.C., Htoon, A.K. and Paterson, J.L. (2007) Alkaline extraction of starch from Australian lentil cultivars Matilda and Digger optimised for starch yield and starch and protein quality. *Food. Chem.* **102**, 551–559.

Lolle, S.J., Hsu, W. and Pruitt, R.E. (1998) Genetic analysis of organ fusion in *Arabidopsis thaliana*. *Genetics*, **149**, 607–619.

Lorenzo, O., Piqueras, R., Sánchez-Serrano, J.-J. and Solano, R. (2003) ETHYLENE RESPONSE FACTOR1 integrates signals from ethylene and jasmonate pathways in plant defense. *Plant Cell*, **15**, 165–178.

Lynn, K., Fernandez, A., Aida, M., Sedbrook, J., Tasaka, M., Masson, P. and Barton, M.K. (1999) The PINHEAD/ZWILLE gene acts pleiotropically in Arabidopsis development and has overlapping functions with the ARGONAUTE1 gene. *Development*, **126**, 469–481.

Matsushita, M., Suzuki, N.N., Fujioka, Y., Ohsumi, Y. and Inagaki, F. (2006) Expression, purification and crystallization of the Atg5–Atg16 complex essential for autophagy. *Acta Crystallographr. F*, **62**, 1021–1023.

Maucher, H., Hause, B., Feussner, I., Ziegler, J. and Wasternack, C. (2000) Allene oxide synthases of barley (*Hordeum vulgare* cv. Salome): tissue specific regulation in seedling development. *Plant J.* **21**, 199–213.

Mayfield, J.A., Fiebig, A., Johnstone, S.E. and Preuss, D. (2001) Gene families from the *Arabidopsis thaliana* pollen coat proteome. *Science*, **292**, 2482–2485.

van Mechelen, J.R., Schuurink, R.C., Smits, M., Graner, A., Douma, A.C., Sedee, N.J., Schmitt, N.F. and Valk, B.E. (1999) Molecular characterization of two lipoxygenases from barley. *Plant Mol. Biol.* **39**, 1283–1298.

Miralles, D.J., Richards, R.A. and Slafer, G.A. (2000) Duration of the stem elongation period influences the number of fertile florets in wheat and barley. *Aust. J. Plant Physiol.* **27**, 931–940.

Mishra, P. and Mohapatra, P.K. (1987) Soluble carbohydrates and floret fertility in wheat in relation to population density stress. *Ann. Bot.* **60**, 269–277.

Muller, J., Wang, Y., Franzen, R., Santi, L., Salamini, F. and Rohde, W. (2001a) In vitro interactions between barley TALE homeodomain proteins suggest a role for protein–protein associations in the regulation of Knox gene function. *Plant J.* **27**, 13–23.

Muller, B.M., Saedler, H. and Zachgo, S. (2001b) The MADS-box gene *DEFH28* from *Antirrhinum* is involved in the regulation of floral meristem identity and fruit development. *Plant J.* **28**, 169–179.

Naik, P.K. and Mohapatra, P.K. (1999) Ethylene inhibitors promote male gametophyte survival in rice. *Plant Growth Regul.* **28**, 29–39.

Nemhauser, J.L., Mockler, T.C. and Chory, J. (2004) Interdependency of brassinosteroid and auxin signaling in Arabidopsis. *PLoS Biol.* **9**, 258.

Nilsson, L., Carlsbecker, A., Sundas-Larsson, A. and Vahala, T. (2007) *APETALA2* like genes from *Picea abies* show functional similarities to their Arabidopsis homologues. *Planta*, **225**, 589–602.

Nonomura, K.I., Nakano, M., Murata, K., Miyoshi, K., Eiguchi, M., Miyao, A., Hirochika, H. and Kurata, N. (2004) An insertional mutation in the rice *PAIR2* gene, the ortholog of *Arabidopsis ASY1*, results in a defect in homologous chromosome pairing during meiosis. *Mol. Genet. Genomics*, **271**, 121–129.

Ohto, M.A., Fischer, R.L., Goldberg, R.B., Nakamura, K. and Harada, J.J. (2005) Control of seed mass by *APETALA2*. *Proc. Natl Acad. Sci. USA*, **102**, 3123–3128.

Okamuro, J.K., den Boer, B.G.W., Lotys-Prass, C., Szeto, W. and Jofuku, K.D. (1996) Flowers into shoots: photo and hormonal control of a meristem identity switch in Arabidopsis. *Proc. Natl Acad. Sci. USA*, **93**, 13831–13836.

Orzaez, D., de Jong, A.J. and Woltering, E.J. (2001) A tomato homologue of the human protein PIRIN is induced during programmed cell death. *Plant Mol. Biol.* **46**, 459–468.

Otsuga, D., DeGuzman, B., Prigge, M.J., Drews, G.N. and Clark, S.E. (2001) *REVOLUTA* regulates meristem initiation at lateral positions. *Plant J.* **25**, 223–236.

Owens, G.P., Hahn, W.E. and Cohen, J.J. (1991) Identification of mRNAs associated with programmed cell death in immature thymocytes. *Mol. Cell. Biol.* **11**, 4177–4188.

Pal, S.K., Takimoto, K., Aizenman, E. and Levitan, E.S. (2006) Apoptotic surface delivery of K^+ channels. *Cell Death Differ.* **13**, 661–667.

Petiot, A., Pattingre, S., Arico, S., Meley, D. and Codogno, P. (2002) Diversity of signaling controls of macroautophagy in mammalian cells. *Cell Struct. Funct.* **27**, 431–441.

Potuschak, T., Vansiri, A., Binder, B.M., Lechner, E., Vierstra, R.D. and Genschik, P. (2006) The Exoribonuclease XRN4 is a component of the ethylene response pathway in Arabidopsis. *Plant Cell*, **18**, 3047–3057.

Price, J., Laxmi, A., St Martin, S.K. and Jang, J.-C. (2004) Global transcription profiling reveals multiple sugar signal transduction mechanisms in Arabidopsis. *Plant Cell*, **16**, 2128–2150.

Prisco, M., Maiorana, A., Guerzoni, C., Calin, G., Calabretta, B., Voit, R., Grummt, I. and Baserga, R. (2004) Role of pescadillo and upstream binding factor in the proliferation and differentiation of murine myeloid cells. *Mol. Cell. Biol.* **24**, 5421–5433.

Sato, T.K., Darsow, T. and Emr, S.D. (1998) Vam7p, a SNAP-25-like molecule, and Vam3p, a syntaxin homolog, function together in yeast vacuolar protein trafficking. *Mol. Cell. Biol.* **18**, 5308–5319.

Sawers, R.J.H., Sheehan, M.J. and Brutnell, T.P. (2005) Cereal phytochromes: targets of selection, targets for manipulation? *Trends Plant Sci.* **10**, 138–143.

Saxena, S.K. and Kaur, S. (2006) Rab27a negatively regulates CFTR chloride channel function in colonic epithelia: involvement of the effector proteins in the regulatory mechanism. *Biochem. Biophys. Res. Commun.* **346**, 259–267.

Shpak, E.D., Berthiaume, C.T., Hill, E.J. and Torii, K.U. (2004) Synergistic interaction of three ERECTA-family receptor-like kinases controls *Arabidopsis* organ growth and flower development by promoting cell proliferation. *Development*, **131**, 1491–1501.

Sláviková, S., Shy, G., Yao, Y., Glozman, R., Levanony, H., Pietrokovski, S., Elazar, Z. and Galili, G. (2005) The autophagy-associated *Atg8* gene family operates both under favourable growth conditions and under starvation stresses in *Arabidopsis* plants. *J. Exp. Bot.* **56**, 2839–2849.

Souer, E., van Houwelingen, A., Kloos, D., Mol, J. and Koes, R. (1996) The *No Apical Meristem* gene of Petunia is required for pattern formation in embryos and flowers and is

expressed at meristem and primordia boundaries. *Cell*, **85**, 159–170.

Sreenivasulu, N., Radchuk, V., Strickert, M., Miersch, O., Weschke, W. and Wobus, U. (2006) Gene expression patterns reveal tissue-specific signaling networks controlling programmed cell death and ABA-regulated maturation in developing barley seeds. *Plant J.* **47**, 310–327.

Steffens, B. and Sauter, M. (2005) Epidermal cell death in rice is regulated by ethylene, gibberellin, and abscisic acid. *Plant Physiol.* **139**, 713–721.

Storey, J.D. and Tibshirani, R. (2003) Statistical significance of genomewide studies. *Proc. Natl Acad. Sci. USA*, **100**, 9440–9445.

Syntichaki, P., Xu, K., Driscoll, M. and Tavernarakis, N. (2002) Specific aspartyl and calpain proteases are required for neurodegeneration in *C. elegans*. *Nature*, **419**, 939–994.

Takumi, S., Kosugi, T., Murai, K., Mori, N. and Nakamura, C. (2000) Molecular cloning of three homoeologous cDNAs encoding orthologs of the maize KNOTTED1 homeobox protein from young spikes of hexaploid wheat. *Gene*, **249**, 171–181.

Tanida, I., Sou, Y.S., Ezaki, J., Minematsu-Ikeguchi, N., Ueno, T. and Kominami, E. (2004) HsAtg4B/HsApg4B/autophagin-1 cleaves the carboxyl termini of three human Atg8 homologues and delipidates microtubule-associated protein light chain 3- and GABAA receptor-associated protein–phospholipid conjugates. *J. Biol. Chem.* **279**, 36268–36276.

Thompson, A.R., Doelling, J.H., Suttangkakul, A. and Vierstra, R.D. (2005) Autophagic nutrient recycling in Arabidopsis directed by ATG8 and ATG12 conjugation pathways. *Plant Physiol.* **138**, 2097–2110.

Trudgill, D.L., Honek, A., Li, D. and Van Straalen, N.M. (2005) Thermal time – concepts and utility. *Ann. Appl. Biol.* **146**, 1–14.

Vaux, D.L. and Hacker, G. (1995) Cloning of mouse RP-8 cDNA and its expression during apoptosis of lymphoid and myeloid cells. *DNA Cell Biol.* **14**, 189–193.

Waddington, S.R., Cartwright, P.M. and Wall, P.C. (1983) A quantitative scale of spike initial and pistil development in barley and wheat. *Ann. Bot.* **51**, 119–130.

Wang, X., Feng, S., Nakayama, N., Crosby, W.L., Irish, V., Deng, X.-W. and Wei, N. (2003) The COP9 signalosome interacts with SCFUFO and participates in Arabidopsis flower development. *Plant Cell*, **15**, 1071–1082.

Wilson, I.D., Barker, G.L.A., Beswick, R.W. *et al.* (2004) A transcriptomics resource for wheat functional genomics. *Plant Biotechnol. J.* **2**, 495–506.

Xiong, Y., Contento, A.L. and Bassham, D.C. (2005) AtATG18a is required for the formation of autophagosomes during nutrient stress and senescence in *Arabidopsis thaliana*. *Plant J.* **42**, 535–546.

Yamagata, H., Uesugi, M., Saka, K., Iwasaki, T. and Aizono, Y. (2000) Molecular cloning and characterization of a cDNA and a gene for subtilisin-like serine proteases from rice (*Oryza sativa* L.) and *Arabidopsis thaliana*. *Biosci. Biotechnol. Biochem.* **64**, 1947–1957.

Yamamoto, Y.Y., Matsui, M., Ang, L.-H. and Deng, X.-W. (1998) Role of a COP1 interactive protein in mediating light-regulated gene expression in Arabidopsis. *Plant Cell*, **10**, 1083–1094.

Yang, M., Wardzala, E., Johal, G.S. and Gray, J. (2004) The wound-inducible *Lls1* gene from maize is an orthologue of the Arabidopsis *Acd1* gene and the LLS1 protein is present in non-photosynthetic tissues. *Plant Mol. Biol.*, **54**, 175–191.

Yemm, E.W. and Willis, A.J. (1954) The estimation of carbohydrates in plant extracts by anthrone. *Biochem. J.* **57**, 508–514.

Yennawar, N.H., Li, L.-C., Dudzinski, D.M., Tabuchi, A. and Cosgrove, D.J. (2006) Crystal structure and activities of EXPB1 (Zea m 1), a β-expansin and group-1 pollen allergen from maize. *Proc. Natl Acad. Sci. USA*, **103**, 14664–14671.

Yip, W.-K., Jiao, X.-Z. and Yang, S.F. (1988) Dependence of in vivo ethylene production rate on 1-aminocyclopropane-1-carboxylic acid content and oxygen concentrations. *Plant Physiol.* **88**, 553–558.

Yoshimoto, K., Hanaoka, H., Sato, S., Kato, T., Tabata, S., Noda, T. and Ohsumi, Y. (2004) Processing of ATG8s, ubiquitin-like proteins, and their deconjugation by ATG4s are essential for plant autophagy. *Plant Cell*, **16**, 2967–2983.

Young, T.E., Gallie, D.R. and DeMason, D.A. (1997) Ethylene-mediated programmed cell death during maize endosperm development of wild-type and shrunken2 genotypes. *Plant Physiol.* **115**, 737–751.

Zheng, H., Ji, C., Li, J., Jiang, H., Ren, M., Lu, Q., Gu, S., Mao, Y. and Xie, Y. (2004) Cloning and analysis of human Apg16L. *DNA Seq.* **15**, 303–305.